J. Astrophys. Astr. (2017) 38: 3
DOI 10.1007/s12036-017-9423-3

Lowering of Asymmetry

K. K. PANDEY[1,*], K. M. HIREMATH[2] and G. YELLAIAH[1]

[1]Department of Astronomy, Osmania University, Hyderabad 500 007, India.
[2]Indian Institute of Astrophysics, Koramangala, Bengaluru 560 034, India.
*Corresponding author. E-mail: pandeyou@yahoo.co.in

MS received 22 April 2016; accepted 2 December 2016; **ePublication**: 14 March 2017

Abstract. Asymmetry, a well established fact, can be extracted from various solar atmospheric activity indices. Although asymmetry is being localized within short time scale, it also persists at different time scales. In the present study we examine the character and nature of asymmetry at various time scales by optimizing the data set, in units of Carrington Rotations (CRs), for Sunspot Area (SA) and soft X-ray flare index (FI_{SXR}). We find from three solar cycles (21-23) that at a small time scale (viz., daily, CRs and monthly) activity appears to be asymmetric with less significance. At larger time scales ($\geq$01 CRs) strength of asymmetry enhances. Number of significant asymmetry points probably depends upon the solar heights. For different combination of data, asymmetry strength appears to be lowered at certain periods $\sim$06, $\sim$12, $\sim$18 CRs (164, 327 and 492 days i.e., harmonics of $\sim$1.3 years. Owing to similar behavior of emergence of magnetic flux, it is conjectured that emergence of flux on the surface probably contributes to the asymmetry of the solar activity.

Keywords. Sun: solar activity—Sun: dynamo—Sun: rotation—Sun: solar flare.

1. Introduction

Symmetry is the foundation of an established dynamic system like Sun and asymmetry evolves during the process leaving an imprint as the occurrence of solar cycle and activity phenomena. Reduction in strength of asymmetry could be the sign of rise in symmetry at specific time/interval. Asymmetry and symmetry, both are inertial effects of some cause, hidden in the solar layers. Asymmetry is an effect in a direction associated with inertia due to internal cause. North–South (N–S) asymmetry of the solar activity is a well recognized phenomenon and is not a random fluctuation (Li *et al.* 2002, 2003). The N–S asymmetries of different activity manifestations have been studied in the past by many authors: the sunspot number and area (Ballester *et al.* 2005; Temmer *et al.* 2006; Zharkov & Zharkova 2006; Zhang & Feng 2015), the number of flares and the flare index (Li *et al.* 1998, 2003; Ozguc *et al.* 2003, 2004), the soft X-ray flare index and disparity in butterfly wing (Pandey *et al.* 2015), and the photospheric magnetic flux (Knaack *et al.* 2005). A statistically significant difference between the levels of solar activity in the northern and southern hemispheres is found by previous studies (Garcia 1990) for several solar activity phenomena. The Sun's N–S asymmetry extends into the solar atmosphere, especially affecting the coronal magnetic equator and the deflection of the heliospheric current sheet (Virtanen & Mursula 2014). The N–S asymmetries of activity phenomena in the solar atmosphere possibly represent important details of the time-dependent part of the magnetic field structure, which is an object of strong interest for the modern dynamo models. Thus, the interest in the N–S asymmetry of solar activity has grown considerably in recent years (Duchlev 2001). Therefore, N–S asymmetry in solar activity is an important physical solar property that needs further detailed investigation (Knaack *et al.* 2005). During a particular period of solar activity, solar magnetic field persists for quite some time (Hathaway *et al.* 1999). It is argued that because of left-handed and right-handed helical magnetic field structures that accumulate in the northern and southern hemispheres separately, conservation of magnetic helicity requires probably that dynamo generated magnetic field be expelled. The mean life time of magnetic flux on the solar surface is 3–6 months (Bieber & Rust 1995). Physics of the N–S asymmetry is not well understood. A possible explanation would be poloidal field generation which may make

one hemisphere stronger than the other hemisphere at the end of a cycle.

The N–S asymmetry has been compared with several other activity parameters that occur in different atmospheric layers of the Sun. All of the above studies leave a wider space to study asymmetry nature on integrated solar disc (i.e., whole disc) at multi-time scales. Data analysis at different time scales like a day, CRs, a month or year categorizes the asymmetry as an imprint of memory. At too short a time scale (a day, a CRs) asymmetry is biased with larger variances (i.e., standard deviation between two data sets). For large time scale (a year or more), nature of asymmetry is suppressed and smeared in smoothing and averaging. A small unit such as CRs is preferably better than monthly unit as it is the time taken by the Sun's surface where the activity is originated. CRs (i.e., Carrington rotation = 27.2753 days of the Earth) is the time taken, in one rotation, by photosphere of the Sun, at the equator. In the present study we find that solar activity asymmetry that persists at all time scales, is an inertial property (i.e., we mean that there exists an internal force that initiates action in a direction) and lower the asymmetry of solar activity at certain periods. The ∼5–6 CRs is a third harmonic of 1.3 years periodicity. Recently, the 1.3-year period is found to be strongly associated with the Indian summer monsoon rainfall (Hiremath *et al.* 2015). There is 5–6 months (150–180 days or ∼7 CRs) phase lag in N–S activity occurrence level that is detected by using sunspot area data by Ravindra & Javaraiah (2015).

This paper is organized as follows. In section 2, we present the rationality for selecting different activity indices and their brief details. The data analysis and results are presented in section 3. In section 4, we discuss in detail the results emerged from the analysis and conclusions in section 5.

2. Data rationality and reduction

Solar activity is a manifestation of temporally and spatially varying distribution of magnetic flux in the photosphere, chromospheres and corona. We use Sunspot Area (SA) indices and, soft X-ray flare index (FI_{SXR}) that occur at solar atmospheric layers and are formed due to different physical conditions. The activity indices can be considered as independently occurring random variables and are measured in both the hemispheres. Sunspot Area (SA) and soft X-ray flare index (FI_{SXR}) are measured values as continuous variables. Such activity indices have different variances at lower time scales but comparable level of variances can be achieved by optimizing the data at higher time scales. A meaningful statistical analysis of any observation requires an optimized data set in terms of the time scales and the physical processes inherent to that observation. The whole data set (01 June1976–31 December 2008) during cycles 21–23, is first separated in two hemispheres. Each date is converted in CRs number and then daily index values are placed (tabled) for CRs of each day. The data for the two hemispheres is binned at increasing time scales (e.g., 01, 02, . . . , 20 CRs). When the daily data is optimized at 01 CRs scale, reduced to 438 samples, 219 at 02 CRs, 146 at 03 CRs, 109 at 04 CRs scale, . . . , 21 at 20 CRs scales as mentioned in column 2 of Table 3. We obtained 20 tables for each of the two data sets (SA and FI_{SXR}) generating a total of $(2 \times 20) = 40$ tables for further analysis. Each table comprises of two populations (Index)N and (Index)S, absolute asymmetry value Δ = N–S, standard deviation of (Index)N, (Index)S as σ_N, σ_S, their difference $\sigma_{diff} = \sigma_N - \sigma_S$, t-value with error probability (α). A brief detail for rationality of selection of these indices are presented below.

- *Sunspot area*[1]: The sunspot numbers are counts of occurrence of sunspots irrespective of whether they are big or small. The Sunspot Area (SA) is rather qualitative (in the sense of their big size or small size or spread) than sunspot numbers. We prefer SA as representative of emerged solar surface magnetic flux for asymmetry study. The daily data of sunspot area are expressed in units of millionths of solar hemisphere.
- *Soft X-ray flare index*[2] (FI_{SXR}): A highly variable, soft X-ray flares are observed by the Earth orbiting Geostationary Operational Environment Satellites (GOES). Antalova (1996) defined the soft X-ray flare index (FI_{SXR}) by weighing the SXR flares of classes B, C, M and X as 0.1, 1, 10 and 100, respectively (i.e., in units of 10^{-6} Wm^{-2}). FI_{SXR} index represents daily variations of SXR flare activity and is a versatile parameter to examine the flare productivity over different temporal and spatial scales (Joshi *et al.* 2015; Abramenko 2005). FI_{SXR} is completely unbiased as different class flares are given proper weightage depending on their peak intensity and therefore FI_{SXR} incorporates the occurrence of every flare, on a particular day, from all the active regions of different sizes and complexities. The FI_{SXR} has been

[1] http://solarscience.msfc.nasa.gov/greenwch.shtml.
[2] http://www.ngdc.noaa.gov/ngdc.html.

used previously, by few authors, to study the variations of flare activity with other physical processes of the Sun (Park *et al.* 2010; Jing *et al.* 2006; Joshi *et al.* 2015).

3. Statistical test for time series

N–S asymmetry significance can be assessed by using student's *t*-test when time series is a non-integer and dimensional (Carbonell *et al.* 2007). While applying this test, with (Index)N and (Index)S, it is a fundamental assumption that the data to be selected from populations have same true variance. The Student's *t*-test is performed using IDL routine TM_TEST. The Student's *t*-test has been used previously to examine the N–S asymmetry of sunspot distribution (e.g., Temmer *et al.* 2006), the N–S asymmetry of FI_{SXR} (Joshi *et al.* 2015). In the present study, we use this test to evaluate the significance of N–S asymmetry in the distribution of FI_{SXR} and SA, at multi-time scales. Since the (Index)N and (Index)S of flare events and sunspot area do not have same true variance (i.e., not Gaussian in distribution), we cannot apply this test.

Therefore, it is useful to first compare and achieve optimum level of the variance of two populations of FI_{SXR}, and SA at increasing time scales with different bin size. For this reason, we perform (a) homogeneity-test of variance of N–S activity and, (b) Gaussian distribution test.

3.1 *Homogeneity test of N–S activity*

Higher correlation coefficient between two populations is a measure of homogeneity of variance. In order to assess homogeneity of variance in N–S activity we plot a scatter-gram as shown in Fig. 1 and calculate correlation coefficient (r). With increasing time scale, correlation coefficient (r) increases as given in Table 1.

3.2 *Gaussian distribution test of variables*

The Gaussian distribution function is as follows:

$$P(x, \mu, \sigma) = \frac{1}{\sqrt{2\pi\sigma^2}} e^{-(x-\mu)/2\sigma^2}, \quad (1)$$

where σ^2 is the variance (or standard deviation σ) in $(\text{Index})_{N+S}$, x is the random values, μ is the mean of $(\text{Index})_{N+S}$ values when data is optimized at 01, 02, 03, ..., 20 CRs. We have 73, 36, 24 random values (data points) for FI_{SXR} and SA at 06, 12, 18 CRs respectively during 1976–2008. Empirically 1σ is equal to 68%. We found $73 \times 68/100 = \sim 49$, $36 \times 68/100 = \sim 25$ and $24 \times 68/100 = \sim 16$ points for two indices. The remaining points are distributed at $\geq 1\sigma$ and $\leq 2\sigma$ levels. It appears that solar activity variations follow the Gaussian distribution, at higher time scales. This shows that variations are strictly a result of a physical process for which the mechanism is not purely random and thus the distribution function appears symmetric about the mean up to 1σ level. We plot Fig. 2 for Gaussian distribution and construct Table 2.

3.3 *Student's t-test of N–S asymmetry*

In our study, initially paired data shows different variance and mean but when the data is optimized at increasing time scales, the different means for (Index)N and (Index)S with comparable variances, are achieved. The above two tests allow to apply the *t*-test at increasing time scales. This test is defined as

$$t = \frac{\bar{D}}{S_{\bar{D}}} = \frac{\frac{(\Sigma D_i)}{n}}{\sqrt{\frac{\Sigma D_i^2 - (\Sigma D_i)^2 / n}{n(n-1)}}}, \quad (2)$$

where D_i is the difference of paired values (index of the northern (Index)N and southern (Index)S hemispheres) and n represents the number of elements that each of the groups have. $\bar{D}$ is the mean of the number of n differences, and $S_{\bar{D}}$ is the respective standard deviation with $n-1$ degrees of freedom (dof). Since we want to test the time scale values (i.e., ~05–06, ~11–12, ~17–18 CRs), n is given by the number of days that fall in different time scales (i.e., 06 CRs $= 6 \times 27.2753 =$ ~163.0). The calculated test value t is compared with error probability α. For error probability $\alpha = 0.01$, 0.05, the difference between the paired values is statistically significant at 99 and 95% levels. Thus for each time scale, *t*-test determines the significance of the difference between the northern and southern hemispheric values and their corresponding standard deviations $S_{\bar{D}}$. The student's *t*-statistic and the corresponding probability of error essentially signify that two populations, (Index)N and (Index)S, have similar variance but significantly different means at higher time scales.

4. Analysis and discussion

4.1 *Exponential reduction in significant N–S asymmetry*

While applying student's *t*-test for different indices (FI_{SXR} and SA) that are binned in 01 to 20 CRs for

the northern and southern hemispheres, the sample size decreases (438, 219, 146, 109, . . . , column 2 of Table 3) with increasing bin size. For two indices FI_{SXR} and SA, we have already generated $2 \times 20 = 40$ tables comprising of N–S asymmetry values, corresponding standard deviation, t-value and probability of error (α). For a more reliable assessment of the true nature of N–S asymmetry, we compared the variance of the two populations at increasing bin size up to 20 CRs and found that the variance (within 100 for FI_{SXR} and 1000 for SA) approaches a similar order at ∼05–06 CRs and onward. FI_{SXR} and SA data series comprise 438 CRs during (1976–2008) for the cycles 21, 22 and 23. When the data is optimized at 01, 02, 03, 04, . . . , 20CRs scales, we have 438/01 = 438, 438/02 = 219, 438/03 = 146, 438/04 = 109, . . . , 21 samples as given in column 2 of Table 3. Now we count the number of significant cases at error probability $\alpha = 0.01$, 0.05 (i.e., at 99%

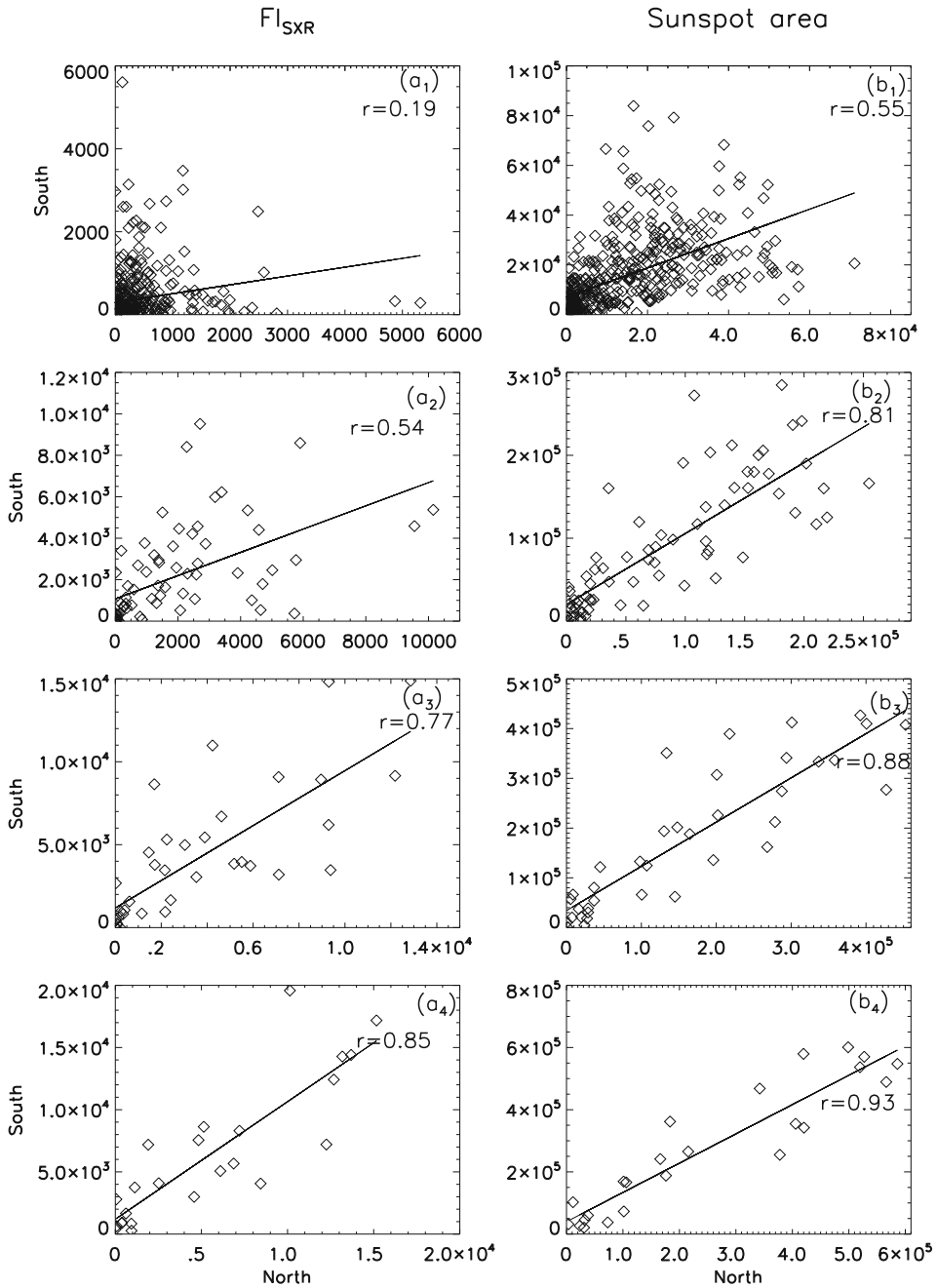

Figure 1. Scatter plots showing correlation between North–South hemisphere values of FI_{SXR} and SA at different time scales. The value of correlation coefficient (r) is mentioned in each panel. Panels (a_1) and (b_1), (a_2) and (b_2), (a_3 and b_3) and, (a_4 and b_4) represent increasing time scales at 01, 06, 12 and 18 CRs respectively.

Table 1. The value of correlation coefficient (r) between two populations (Index)N and (Index)S for FI_{SXR} and SA at increasing time scales of 01, 6, 12, and 18 CRs during the cycles 21, 22 and, 23.

CRs	FI_{SXR}	Sunspot area
01 CRs	0.19	0.55
06 CRs	0.54	0.81
12 CRs	0.77	0.88
18 CRs	0.85	0.93

and 95% confidence levels) for every binning and then calculate the percentage strength of cases for that particular bin. At 01 CRs scale, out of 438 samples, we get 57 cases at 99% significance and its percentage strength is 57/438 × 100% = 13%. At 02 CRs scale, out of 219 samples, we get 45 cases at 99% significance and its percentage strength is 45/219 × 100% = 20.45%. Similarly at 03 CRs, out of 146 samples, 36 cases are at 99% significance, percentage strength 36/146 × 100% = 24.66%. Table 3 (columns 1, 2, 3, 4, 5, 6 . . . × 20 rows), in which, the percentage strength, 13%, 20.45%, 24.66% . . . , of asymmetry are given in bracket. We interpret it as 13%, 20.45%, 24.66% . . . , of the Carrington rotation values, during cycle 21–23, and are asymmetric at the 99% significance level in terms of FI_{SXR}.

We plot the number of significant asymmetry cases given in column 3 of Table 3, marked as 'A' (e.g., for FI_{SXR}: 57, 45, 36, . . . , corresponding to 01, 02, 03, . . . , 20 CRs) at 99% and, column 4 marked as 'B' (e.g., for FI_{SXR}: 135, 85, 61,46, 36, 38, . . . , corresponding to 01, 02, 03, . . . , 20 CRs) at 95% significance levels which exponentially decreases as shown in the upper panel of Fig. 3 by lines A (solid-diamond) and B (dashed-asterisk).

Table 2. Mean (μ) and standard deviation (σ) of FI_{SXR} and SA indices optimized at 06, 12, 18 CRs during cycles 21, 22 and 23.

		Cycle 21, 22, 23	
Indices	CRs	Mean	1σ
FI_{SXR}	06	3835	3831
	12	7567	7282
	18	11666	10354
Sunspot area	06	170719	140066
	12	336824	274461
	18	519193	402540

We over-plot the percentage strength of asymmetry given in brackets in column 3 of Table 3 marked as 'P' (e.g., for FI_{SXR}: 13.01, 20.55, 24. 66, . . . , corresponding to 01, 02, 03, . . . , 20 CRs) at 99% and, column 4 marked as 'Q' (e.g., for FI_{SXR}: 30.82, 38.81, 41.78, 42.20, 41.38, . . . , corresponding to 01, 02, 03, . . . , 20 CRs) at 95% significance levels as the curves are marked by 'P' and 'Q' in the upper panel of Fig. 3. We observe that the percentage strength, 13%, 20.45%, 24.66% . . . , an incremental nature lowers down at ∼05–06 CRs. The similar reduction is observed at ∼12 and ∼18 CRs. It is interesting to note that percentage value increases and strengthens till ∼05–06 CRs and falls, then it rises with fluctuation till ∼11 CRs and falls at ∼12 CRs. Similarly the trend is repeated for ∼18 CRs. On these

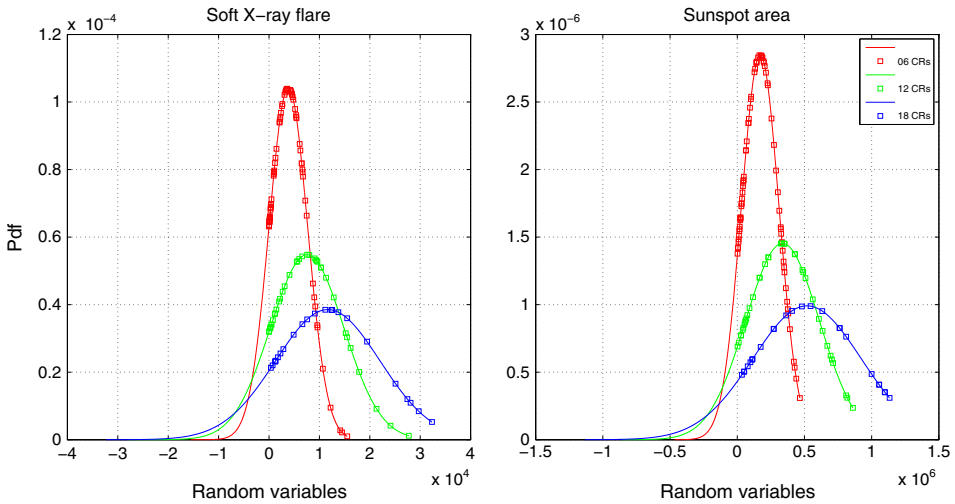

Figure 2. Gaussian distribution of (**a**) soft x-ray flare Index (FI_{SXR}), (**b**) sunspot area (SA) indices when data is optimized at 06, 12 and 18 CRs scale indicated by red, green and blue line-squares respectively. Mean (μ) and standard deviation (σ) for each panel are given in Table 2. X-axis represents the random variables (i.e., data values) and Y-axis the probability density function.

Table 3. Significant points observed on various time scales (in units of CRs) for FI_{SXR}, sunspot area, at 99 and 95% significance levels. Values in brackets of columns 3 to 6 are percentage of asymmetry plotted in Fig. 3 marked by P and Q.

		FISXR		Sunspot area	
CRS (1)	Sample (2)	(3) 99%	(4) 95%	(5) 99%	(6) 95%
–	–	A (P)	B (Q)	A (P)	B (Q)
01	438	57(13.01)	135(30.82)	245(55.94)	283(64.61)
02	219	45(20.55)	85(38.81)	131(59.58)	155(70.78)
03	146	36(24.66)	61(41.78)	89(60.96)	102(69.86)
04	109	28(25.69)	46(42.20)	71(65.14)	82(75.23)
05	87	23(26.44)	36(41.38)	50(57.47)	54(62.07)
06	73	17(23.29)	38(52.05)	42(57.53)	52(71.23)
07	62	17(27.42)	28(45.16)	35(56.45)	43(69.35)
08	64	15(27.78)	21(38.89)	33(61.11)	37(68.52)
09	48	14(29.17)	21(43.75)	32(66.67)	33(68.75)
10	43	13(30.23)	24(55.81)	28(65.12)	31(72.09)
11	39	11(28.21)	18(46.15)	29(74.36)	31(79.49)
12	36	09(25.00)	15(41.67)	24(66.67)	25(69.44)
13	33	10(30.30)	16(48.48)	27(81.82)	29(87.88)
14	31	07(22.58)	19(61.29)	21(67.74)	23(74.19)
15	29	10(34.48)	15(51.72)	20(68.97)	24(82.76)
16	26	07(26.92)	12(46.15)	15(57.69)	20(76.92)
17	26	06(23.08)	10(38.46)	12(46.15)	16(61.54)
18	24	06(25.00)	9(37.50)	17(70.83)	19(79.17)
19	23	04(17.39)	10(43.48)	13(56.52)	17(73.91)
20	21	04(19.05)	9(42.86)	16(76.19)	16(76.19)

lines P, Q, the observed depression indicated by arrow marks at ∼05–06, ∼12, ∼18 CRs are probably the time when asymmetry lowers.

4.2 *Difference of standard deviation as N–S asymmetry*

N–S asymmetry of solar activity is generally understood and defined by the difference of northern (N) and southern (S) hemispheric index as absolute asymmetry Δ = N–S which generates correct asymmetry time series. However, normalized asymmetry of solar activity index, defined as Δ = N–S/ N+S, is misleading (Ballester *et al.* 2005). These traditional methods are used, in all the studies of asymmetry, to find the relative differences between two hemispheric activities when the data is binned over a day, month or year. It does not provide any suggestion of internal changes in solar interior within that time scale. Standard deviation values reveal dynamical phenomena (high variability of activity in two hemispheres) along the cycle (Feminella & Storini 1997). The difference of standard deviation (σ_{diff}) corresponding to the absolute asymmetry index 'Δ' at a particular time interval signifies the level of fluctuation in the data sample. It is also suggestive of changes in the solar interior dynamics within a specific time interval. By using difference of standard deviation ($\sigma_{diff} = \sigma_N - \sigma_S$) with increasing bin sizes from 01 CR to 20 CRs could provide useful information for understanding the solar interior within specific time scales. It should be noted that, in general, σ is positive whereas in our case σ_{diff} could be positive (North) or negative (South). Figure 4 illustrates the N–S asymmetry as localized changes in terms of σ_{diff} at different time scales. This kind of representation (i.e., σ_{diff} plot) may be very useful to understand the persistence of hemispheric occurrence of solar activity during various phases of the solar cycle.

There appears to be an excellent correlation between variation in FI_{SXR} (at coronal heights) and SA (at surface) time series, but on close examination (i.e., σ_{diff} plot with Δ = N–S), the panels (a), (b), (c), (d) in Fig. 5, we find that each significant asymmetry in SA (panel (c)) does not coincides with FI_{SXR}(panel (a)). Significant asymmetry points of SA index are more than (Fig. 5 and Table 3) that of FI_{SXR} at coronal heights. In Fig. 5, we observe that out of 38 significant points of FI_{SXR} (panels (a) and (b)) only 30 points (diamond) have one-to-one correspondence with panels (c) and (d) having 52 significant points of SA at ∼06 CRs scale. At ∼12 CRs scale, out of 15 points of FI_{SXR} (panels (a), (b)) only 13 points (asterisk) have one-to-one

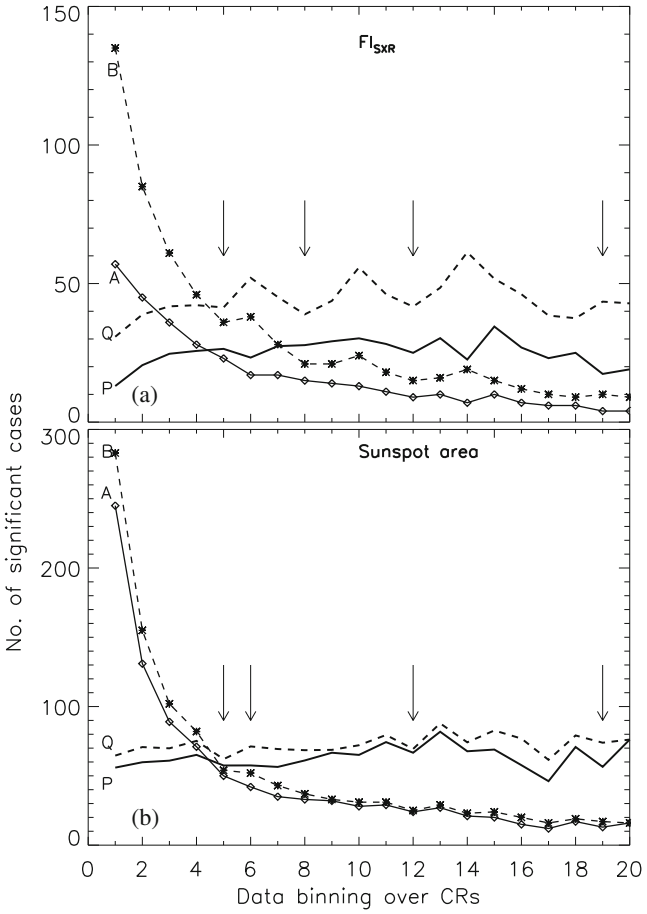

Figure 3. Exponential decrease in the number of significant N–S asymmetry cases with increasing time scale, in units of CRs, is represented by curve 'A' (solid line-diamonds) at 99% and curve 'B' (dashed line – asterisks) at 95%. At the bottom two horizontal curves 'P' (thick solid line) and 'Q' (thick dashed line) are percentage strengths of N–S asymmetry, the arrow marks indicating the lowered asymmetry.

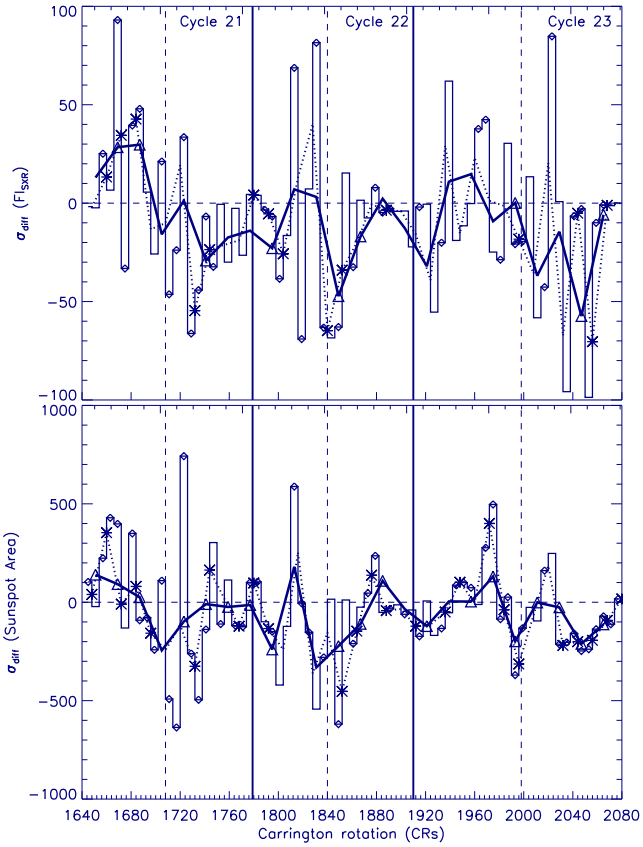

Figure 4. Plot representing N–S asymmetry as difference of standard deviation σ_{diff} in (**a**) FI_{SXR} and (**b**) sunspot area corresponding to significant N–S absolute asymmetry (Δ = N–S) at 06 (histogram line – diamonds), 12 (dotted line – asterisks) and 18 (solid thick line – triangles) CRs respectively. Dashed vertical lines indicate the times of solar maximum.

correspondence with panels (c) and (d) having 25 significant points. At 18 CRs scale, 9 out of 9 points of FI_{SXR} (panels (a) and (b), triangles) have one to one correspondence with panels (c) and (d) having 19 significant points. It appears that all significant variation at solar surface is not connected with a distant corona. The soft X-ray emission from a magnetic loop system in coronal region appears to depend virtually linearly on magnetic flux through the photospheric surface area magnetically connected with that of the corona (Schrijver 1987). In other words the emission from a coronal magnetic loop depends linearly on the intensity of magnetic field structure i.e., probably anchored in the convection zone (Rutten & Schrijver 1994).

During cycle 21, asymmetry is shifted from north to south and remains there till cycle 23 as explained in previous studies, is distinctly seen in Fig. 5 (at 18 CR$_S$, the thick line – triangles).

5. Concluding remarks

The present study examines the nature of asymmetry at different time scales and it appears from Table 3 and Figures 3–5 that

(i) there is substantial difference in the number of asymmetry points between FI_{SXR} and SA at 99 and 95% significance levels;
(ii) every significant disturbance/deviation in magnetic activity at photosphere does not result in a significant asymmetry at coronal heights;
(iii) at ~06, ~12 and ~18 CRs, strength of significant asymmetry is lowered (i.e., hidden or underlying symmetry increases). In other words, the lowering of asymmetry cannot happen without cause or

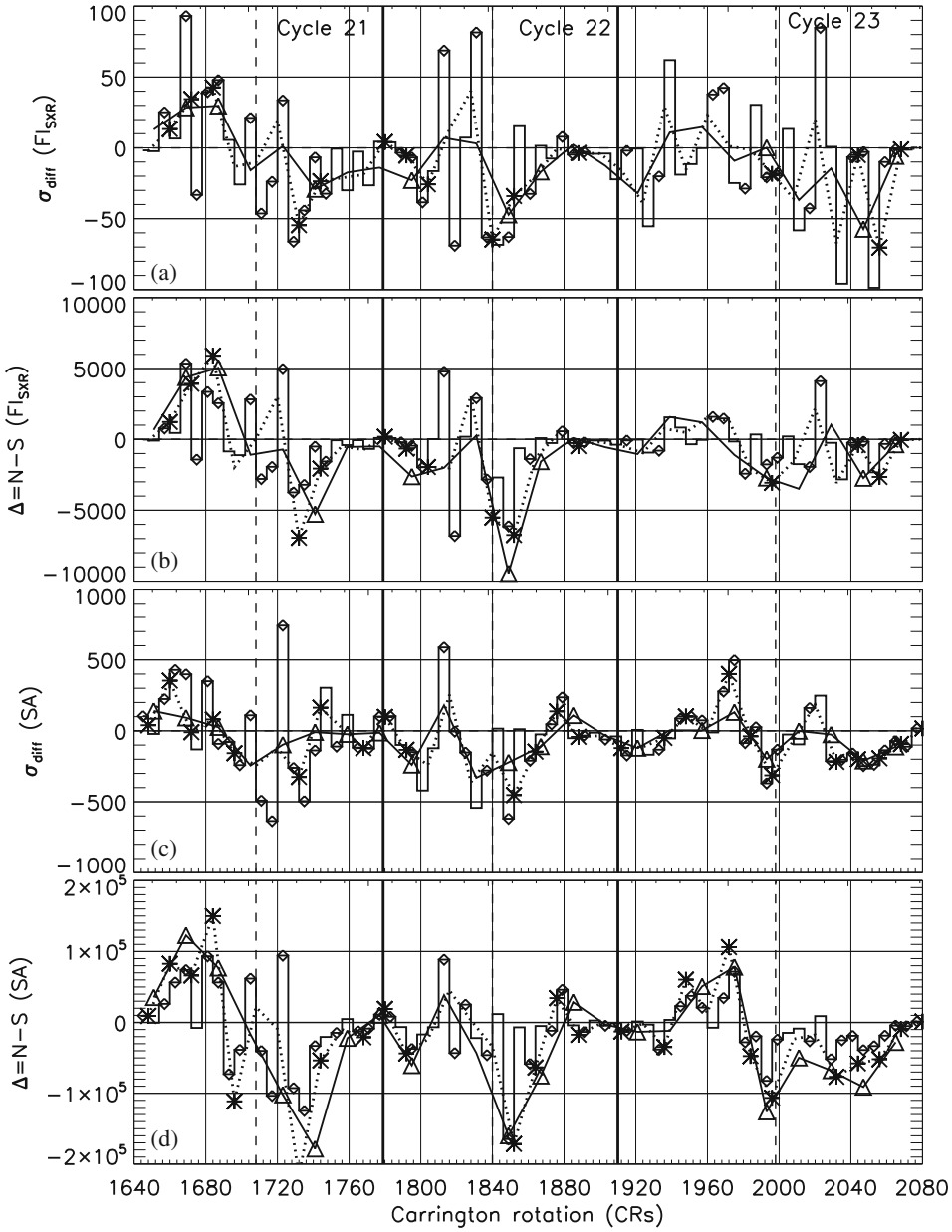

Figure 5. Difference of standard deviation (σ_{diff}) plot representing 95% significant N–S asymmetry in (**a**) FI_{SXR} and (**c**) sunspot area corresponding to 95% significant absolute (Δ = N–S) asymmetry (panels (**b**), (**d**)) at 06 (histogram line – diamonds), 12 (dotted line – asterisks) and 18 (solid thick line – triangles) CRs. Dashed vertical line indicates the time of maximum.

symmetry cannot originate spontaneously against inertia of asymmetry. At these periods either magnetic flux enhances in the opposite direction to counter the asymmetry or excess of accumulated magnetic flux defuses towards the pole. In other words, when the leading edges of the N and S equator-ward propagating toroidal bands come within a closest range for interaction and flux cancellation, an active coupling occurs deep in the interior (Norton *et al.* 2014).

Differential rotation of the Sun is one of the main ingredients of the solar dynamo located at the base of the convection zone, which is believed to generate the magnetic field structure observed at the solar surface. Recent helioseismic probing of solar interior has shown that rotation rate of the Sun near the base of the convective zone changes with a period of roughly 1.3 years (Howe *et al.* 2000). The presence or absence of this periodicity (∼05–06, ∼12, ∼18 CRs as harmonics of 1.3 years) in solar surface data would strengthen

or weaken the case for associated changes in the layers harbouring the dynamo.

It is expected that any fluctuation in the dynamo process will manifest on the surface as freshly emerged flux, i.e. in young active regions (Krivova & Solanki 2002). The mean life time of magnetic flux on the solar surface is 3–6 months (Bieber & Rust 1995). It is to be noted that 05-06 CRs period of asymmetric activity is equal to ∼135–165 days or within 3–6 months. The generation of magnetic flux of this duration may be one of the causes for the enhancement of asymmetry. Variations in activity within the period of 150–160 days or 156 days are detected in the occurrence of high-energy solar flares (Rieger *et al.* 1984), and also in the sunspot areas (Carbonell & Ballester 1990, 1992). It is interesting to note that whether by coincidence or not, 150–160 days correspond to ∼05–06 CRs. Hence it is not surprising that the solar activity around ∼05–06, ∼12, ∼18 CRs (with periodicity of ∼156, ∼312 ∼468 days) gets enhanced.

Asymmetry of solar activity at different layers strengthens, initially up to ∼05 CRs, when the short term variations are averaged. A hidden symmetry emerges in solar activity about which solar dynamics displays asymmetry phenomena. We found similar results when larger data set of sunspot area is analysed. It, however, needs to be examined on other data sets too. Regularity of natural law is exhibited as symmetry during dynamical processes and any variation/fluctuation from regularity is an indicator of asymmetric phenomena hidden probably at the base of the convection zone. On the other hand, generation of magnetic flux at duration of 3–6 months and its relationship with increase in solar activity indices are beyond the scope of this study.

Acknowledgements

The authors are grateful to the anonymous referees for useful and constructive comments that substantially improved this manuscript. One of the authors (KKP) gratefully acknowledges the HoD, Department of Astronomy, Osmania University for providing infrastructural support.

References

Abramenko, V. I. 2005, *ApJ*, **629**, 1141.
Antalova, A. 1996, *Contributions of the Astronomical Observatory Skalnate Pleso*, **26**, 98.
Ballester, J. L., Oliver, R., Carbonell, M. 2005, *A&A*, **431**, L5.
Bieber, J. W., Rust, D. M. 1995, *ApJ*, **453**, 911.
Carbonell, M., Terradas, J., Oliver, R., Ballester, J. L. 2007, *A&A*, **476**, 951.
Carbonell, M., Ballester, J. L. 1990, *A&A*, **238**, 377.
Carbonell, M., Ballester, J. L. 1992, *A&A*, **255**, 350.
Duchlev, P. I. 2001, *Sol. Phys.*, **199**, 211.
Feminella, F., Storini, M. 1997, *A&A*, **322**, 311.
Garcia, H. A. 1990, *Sol. Phys.*, **127**, 185.
Hathaway, D. H., Wilson, R. M., Reichmann, E. J. 1999, *J. Geophys. Res.*, **104(22)**, 375.
Hiremath, K. M., Hegde, M., Soon, W. 2015, *New Astronomy*, **8**, 13.
Howe, R., Christensen-Dalsgaard, J., Hill, F., Komm, R. W., Larsen, R. M., Schou, J., Thompson, M. J., Toomre, J. 2000, *Science*, **287**, 5456.
Jing, J., Song, H., Abramenko, V., Tan, C., Wang, H. 2006, *ApJ*, **644**, 1273.
Joshi, B., Bhattacharyya, R., Pandey, K. K., Kushwaha, U., Moon, Y.-J. 2015, *A&A*, 582.
Knaack, K., Stenflo, J. O., Berdygina, S. V. 2005, *A&A*, **438**, 1067.
Krivova, Solanki 2002, *A&A*, **394**, 701.
Li, K. J., Wang, J. X., Xiong, S. Y., Liang, H. F., Yun, H. S., Gu, X. M. 2002, *A&A*, **383**, 648.
Li, K.-J., Schmieder, B., Li, Q.-S. 1998, *A&A*, **131**, 99.
Li, K. J., Wang, J. X., Zhan, L. S., Yun, H. S., Liang, H. F., Zhao, H. J., Gu, X. M. 2003, *Sol. Phys.*, **215**, 99.
Norton, A. A., Charbanneu, P., Passos, D. 2014, *Space Sci. Rev.*, **186**, 251.
Ozguc, A., Atac, T., Rybak, J. 2003, *Sol. Phys.*, **214**, 375.
Ozguc, A., Atac, T., Rybak, J. 2004, *Sol. Phys.*, **223**, 287.
Pandey, K. K., Yellaiah, G., Hiremath, K. M. 2015, *Ap&SS*, **356**, 215.
Park, S.-H., Chae, J., Wang, H. 2010, *ApJ*, **718**, 43.
Ravindra, B., Javaraiah, J. 2015, *New Astronomy*, **39**, 55.
Rieger, E., Share, G. H., Forrest, D. J., Kanbach, G., Reppin, C., Chupp, E. L. 1984, *Nature*, **312**, 623.
Rutten, R. J., Schrijver, C. J. (eds) 1994, *Solar surface magnetism*, Kluwer.
Schrijver, C. J. 1987, *A&A*, **180**, 241.
Temmer, M., Rybak, J., Bendik, P., Veronig, A., Vogler, F., Otruba, W., Potzi, W., Hanslmeier, A. 2006, *A&A*, **447**, 735.
Virtanen, I. I., Mursula, K. 2014, *ApJ*, **781**, 99.
Zharkov, S., Zharkova, V. V. 2006, *Adv. Space Res.*, **38**, 868.
Zhang, J., Feng, W. 2015, *AJ*, **150**, 74.